^{14}N Mims Pulsed-ENDOR of Proximal Histidine and Heme of Aquometmyoglobin and Fluorometmyoglobin

Hong-In Lee

Department of Chemistry Education, Kyungpook National University, Deagu 702-701, Korea
Received October 11, 2002

Previous ^{19}F and $^{1,2}H$ electron-nuclear double resonance (ENDOR) study of fluorometmyoglobin (MbF) in frozen-solution state provided sensitive tools sensing subtle structural changes of the heme that are not obtainable from X-ray. [Fann *et al., J. Am. Chem. Soc.* **1995**, *117*, 6019] Because of the intrinsic inhomogeneouse EPR line broadening effect of MbF in frozen-solution state, detection of the electronic and geometrical changes of the heme ring itself and the proximal histidine by using ^{14}N CW ENDOR was interfered. In the present study, hyperfine-sensitive ^{14}N Mims ENDOR technique of pulsed-EPR was employed to probe the changes. With two different τ values of 128 and 196 ns, ^{14}N ENDOR signals of the heme and proximal histidine were completely resolved at $g'_{\parallel}$ (= g_e = 2). This study presents that X-band ^{14}N Mims ENDOR sequence can sensitively detect the small changes of the spin densities and p orbital populations of the proximal and the heme nitrogens, caused by ligand and pH variation of the distal site.

Key Words : Metmyoglobin, ENDOR, Mims ENDOR, ^{14}N hyperfine, High-spin Fe(III)

Introduction

Heme-containing proteins are essential for metabolic cycles of lives in many biological systems by doing dioxygen transport, electron transfer, and other catalytic functions.[1] The active site, heme, consists of iron ion, heme ring, endogenous ligand (or proximal pocket), and exogenous ligand binding site (or distal pocket). Because ligand binding at the distal pocket of the heme is the key for the functions of the hemoproteins, characterizing and controlling of ligand binding at the distal pocket have been of interest for many decades.[1] Electron paramagnetic resonance (EPR) techniques are often used to probe changes of the distal pocket by using several different kinds of ligand, such as F^-, CN^-, and N_3^-, which are able to bind to the exogenous ligand binding site of iron ion.[2-6] They measure the nuclear hyperfine couplings of the axial ligands to detect subtle structural changes of the pocket.

It is expected that changes of chemical environments at the distal site affect the electronic and geometrical structures of the heme ring itself and the proximal site. Previous ^{19}F continuous-wave (CW) and pulsed electron-nuclear double resonance (ENDOR) of fluorometmyoglobin (MbF) was shown to be sensitive to structural changes of the distal heme pocket which are not obtainable through other spectroscopical methods.[4] However, probing the changes at the heme ring and the proximal histidine was interfered because the changes at the heme ring and the proximal site are rather small and MbF in frozen-solution state intrinsically gives rise to inhomogeneouse EPR line broadening. Present study employs hyperfine-selective ^{14}N Mims ENDOR technique[7] of pulsed-EPR to resolve ^{14}N hyperfine couplings of the heme and the proximal histidine and to probe the subtle changes of the spin densities and p orbital populations of the proximal and the heme nitrogens, caused by ligand and pH variation of the distal site in metmyoglobin (Mb^+) and MbF.

*Phone: +82-53-950-5904, Fax: +82-53-950-5899, E-mail: leehi@knu.ac.kr

Experiments and Theory

Sample preparation. Horse ferric myoglobin (Mb^-) was obtained from Sigma Chemical Co. and used without further purification. 1-2 equivalents of ferricyanide were added to ensure complete oxidation. Remaining ferri- and ferrocyanide were removed from the protein solution by washing the solution with several volumes of working buffer (50 mM potassium phosphate at pH 6) using microconcentrators. The protein solution was diluted with 0.2 M potassium fluoride to prepare fluorometmyoglobin (MbF) in the buffer solution of desired pH and concentrated to greater than 2 mM with Centricon microconcentrators. All aqueous buffers contained 60% (v/v) glycerol. Sample concentrations were spectroscopically determined (Hewlett-Packard 8451A diode array spectrophotometer) using $\varepsilon_{408}(Mb^-)$ = 188 $mM^{-1}cm^{-1}$ and $\varepsilon_{408}(MbF)$ = 146 $mM^{-1}cm^{-1}$.[1,8]

EPR and ENDOR measurements. Q-band (35 GHz) CW EPR and ENDOR spectra were collected on a modified Q-band Varian E-109 spectrometer equipped with a liquid helium immersion dewar, described previously.[9] The spectra were recorded at 2 K in dispersion-mode under rapid-passage condition under which EPR spectra represent actual absorption envelope.[10,11] Mims ENDOR experiments[7] were performed locally-built X-band (9 GHz) pulsed-EPR spectrometer, previously described in detail.[12] Stimulated-echo pulse sequence ($\pi/2$ - τ - $\pi/2$ – T - $\pi/2$ - τ - echo) was employed to collect Mims ENDOR data.[13,14] Electron spin echo intensities were recorded at 2 K as a function of radio frequency (RF) which was applied during the time interval,

T. between the second and the third microwave pulses. The widths of $\pi/2$ microwave pulse and RF pulse were 16 ns and 15 μs. respectively.

ENDOR frequencies. EPR and ENDOR spectra of a high-spin Fe(III) (S = 5/2) system coupled to a nucleus with a nuclear spin I (I ≠ 0) are described by the spin Hamiltonian consisting of the fine structure (zero-field splitting), the electron and nuclear Zeeman interactions. the nuclear hyperfine interaction, and the nuclear quadrupole interaction as[15]

$$\boldsymbol{H} = \mathbf{S}\cdot\mathbf{D}\cdot\mathbf{S} + g_e\beta\mathbf{B}\cdot\mathbf{S} - g_N\beta_N\mathbf{B}\cdot\mathbf{S} + \mathbf{S}\cdot\mathbf{A}\cdot\mathbf{I} + \mathbf{I}\cdot\mathbf{P}\cdot\mathbf{I}. \quad (1)$$

Here, **S**. **D**. g_e, β. **B**. g_N. β_N. **A**. **I**. and **P** refer to the electron spin, the zero-field splitting (ZFS) tensor. the electronic g factor. the Bohr magneton, the applied magnetic field, the nuclear g factor. the nuclear magneton, the hyperfine tensor. the nuclear spin. and the nuclear quadrupole tensor for I ≥ 1. respectively. Six (= 2S+1) electron-spin eigenstates of the high-spin Fe(III) system are splitted into three Kramers doublets (m_S = ±1/2. ±3/2, ±5/2). of which m_S = ±1/2 doublet is the lowest for D > 0, at zero magnetic field by the ZFS tensor which is characterized by the axial and rhombic ZFS parameters. D and E.

For Mb^- and MbF with axial ZFS tensor (E = 0). the energy separation. 2D, between m_S = ±1/2 and m_S = ±3/2 doublets are ~19 cm^{-1} and ~12 cm^{-1}, respectively.[3,4] These separations are large. compared to the electronic Zeeman energy at the experimental X- (9 GHz) and Q-bands (35 GHz), so that the EPR and ENDOR spectra of Mb^+ and MbF arise only from the lowest Kramers doublet. m_S = ±1/2. In this case. the m_S = ±1/2 doublet of the above S = 5/2 spin system (eq. (1)) can be treated as an effective spin S' = 1/2 system which can be described by an effective spin Hamiltonian.[15]

$$\boldsymbol{H'} = \beta\mathbf{S'}\cdot\mathbf{g'}\cdot\mathbf{B} + \beta_N\mathbf{I}\cdot\mathbf{g}^N\cdot\mathbf{B} + \mathbf{S'}\cdot\mathbf{A'}\cdot\mathbf{I} + \mathbf{I}\cdot\mathbf{P}\cdot\mathbf{I}. \quad (2)$$

where **g'** and **A'** are the orientation-dependent **g**- and hyperfine tensors in the effective spin representation. Though the **g**-tensor of S = 5/2 spin system in eq. (1) is typically considered as isotropic. the **g'**-tensor. which is coaxial with the ZFS tensor. of the S' = 1/2 fictitious spin representation (eq. (2)) is axial with $g'_\parallel = g_e = 2$ and $g'_\perp = 3g_e = 6$. The hyperfine tensor in the effective spin representation is given by $\mathbf{A'} = \mathbf{A}\cdot(\mathbf{g'}/g_e)$. $\mathbf{g}^N$ is an effective nuclear g tensor which is also coaxial with the ZFS tensor.

Because the selection rule for ENDOR transition is Δm_S = 0 and Δm_I = ±1. ENDOR spectrum can be explained by the second. third. and fourth terms in the right side of eq. (2). giving ENDOR frequencies explicitly expressed as[15,16]

$$\nu_\pm(m_I) = |\pm A'/2 + \nu_N + 3P(2m_I-1)/2|. \quad (3)$$

Here, A' (=Ag'/g_e) is the angle-dependent hyperfine coupling constant in S' = 1/2 representation. P is the angle-dependent nuclear quadrupole coupling constant. and I ≥ m_I ≥ –I + 1. ν_N is the nuclear Larmor frequency which is given by $g^N\beta_N B_o/h$.[17] The nuclear quadrupole splitting Hamiltonian is expressed by traceless three principle values. P_{11}. P_{22}. and P_{33} ($P_{11} + P_{22} + P_{33} = 0$). where P_{ii} values are determined by two independent parameters: the largest component. $P_{33} = eq_iQ/[2hI(2I-1)]$. and the asymmetry parameter. $\eta = (P_{11}-P_{22})/P_{33}$. Here. eq_i is the electric field gradient, Q is the nuclear quadrupole moment. and 1 ≥ η ≥ 0.

Results and Discussion

EPR spectra of both frozen-solution high-spin Fe(III) Mb^- and MbF at 2 K show axial signals with $g'_\parallel = g_e = 2$ and $g'_\perp = 3g_e = 6$ where the $g'_\parallel$ axis is normal to the heme plane.[2,4] In MbF, axial H_2O ligand of the native Mb^- is replaced with F^- upon fluorination, which gives additional resolution from ^{19}F hyperfine coupling of ~46 G at $g'_\parallel$ on EPR of MbF. EPR study on MbF crystal had observed a slight rhombicity,[18,19] but we could not resolve further in our frozen-solution EPR because of large inhomogeneous line broadening.

Figure 1 shows "single-crystal-like" ^{14}N Q-band (35 GHz) CW ENDOR signals obtained at $g'_\parallel$ of the EPR envelopes of Mb^+ and MbF. These ^{14}N signals arise from four heme nitrogens and N_ε of the proximal histidine.[2,20] The signals are not well resolved except for the signals at 10.5-11.5 MHz. which are assigned to the proximal histidine N_ε nitrogen.[2,20] From eq. (3), one can expect four ENDOR lines from each ^{14}N nucleus (I = 1). Therefore, total eight ^{14}N ENDOR lines are expected if we assume hyperfine couplings of four heme nitrogens are identical.[21] However, in Q-band CW ENDOR, ν_- doublet are not often seen because of delicate balance of relaxation.[16] Furthermore, overlapping of ENDOR lines reduces the number of observed ENDOR bands to three or four. This reduction of the number of the observed lines hampers the accurate analysis of the hyperfine and the nuclear quadrupole couplings of the heme and proximal

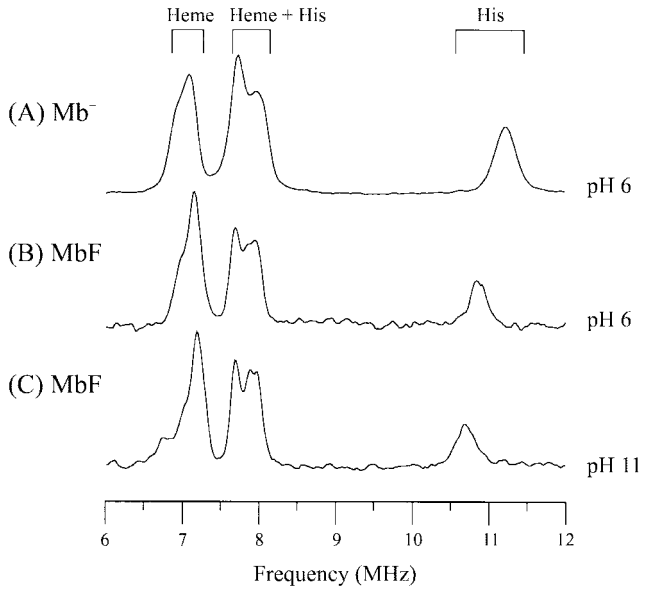

Figure 1. Q-band (35 GHz) CW ENDOR spectra at g' = 2.00 of (A) Mb^+ (pH 6), (B) MbF (pH 6), and (C) MbF (pH 11). *Experimental conditions:* microwave frequency, (A, B) 35.055 GHz, (C) 35.051 GHz; modulation amplitude, 0.67 G; modulation frequency, 100 kHz; rf scan speed, 0.5 MHz/s; time constant, 64 ms.

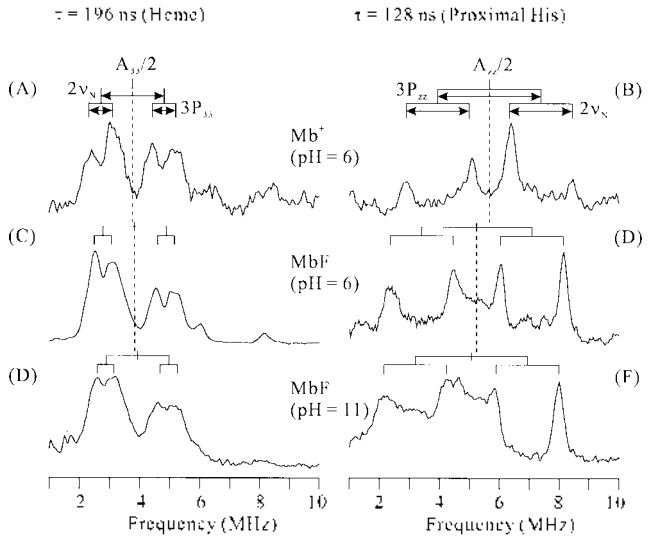

Figure 2. X-band (9 GHz) Mims ENDOR spectra at g' = 2.00 of (A, B) Mb^- (pH 6), (C, D) MbF (pH 6), and (E,F) MbF (pH 11). *Experimental conditions:* microwave frequency, (A, B) 9.401 GHz GHz, (C, D) 9.463 GHz, (E, F) 9.479 GHz; τ, (A, C, E) 196 ns, (A, C, E) 128 ns; shot repetition rate, 100 Hz. Other experimental conditions are described in experimental section.

histidine nitrogens.

Mims ENDOR is known to be hyperfine-selective and its ENDOR response is depending on the hyperfine coupling, A, and the time interval, τ, between the first and the second microwave pulses as following.[11,13,22,23]

$$R \propto [1-\cos(2\pi A\tau)] \quad (4)$$

As in the above equation, the ENDOR response is zero for $A\tau$ = 1, 2, ... and maximum for $A\tau$ = 1/2, 3/2, ... Using the hyperfine-selectivity of Mims ENDOR, attempts for separating ^{14}N ENDOR of the heme nitrogen and the nitrogen of the proximal histidine were made. Figure 2 shows Mims ENDOR spectra obtained at $g'_{\parallel}$ of Mb^+ and MbF with two different τ values, 128 and 196 ns. From eq. (4), τ = 128 ns maximizes ENDOR signal with A = 3.9, 11.7, ... MHz and minimizes ENDOR with A = 7.8, 15.6, ... MHz. And τ = 196 ns maximizes ENDOR signal with A = 2.6, 7.7, ... MHz and minimizes ENDOR with A = 5.1, 10.2, ... MHz. As seen in figure 2, each Mims ENDOR spectrum shows distinct four-line ENDOR pattern centered at A/2 and separated by 3P, nuclear quadrupole coupling, and $2\nu_N$, twice the ^{14}N Larmor frequency (eq. (4)). Based on previous ENDOR of Mb^+,[2,20] we assign ENDOR signals with τ = 196 ns and τ = 128 ns to ^{14}N of the heme and N_ε of the proximal histidine, respectively. Because ENDOR spectra were obtained at $g'_{\parallel}$, the magnetic field is normal to the heme plane so that the measured hyperfine and the nuclear quadrupole couplings are the tensor components along that direction: heme normal for heme nitrogens and Fe-N_ε bond direction for the histidine nitrogen. These observed coupling tensor components are listed in Table 1.

The ^{14}N coupling values of this work are in good agreement with those of Mb^- previously reported from crystal (Table 1). Our frozen-solution data show a slight discrepancy of the values between the crystal data and our work. This is in part large inhomogeneous line broadening of EPR.[19] As seen in the figure 2 and table 1, when Mb^+ is fluorinated and pH of MbF is increased, the ^{14}N hyperfine couplings change sensitively. Previous ENDOR study of MbF did not recognized the change of ^{14}N hyperfine and nuclear quadrupole couplings.[4] However, even though the changes of the ^{14}N hyperfine and the nuclear quadrupole couplings are very small, current measurements using X-band Mims ENDOR clearly resolved the heme and the proximal histidine ^{14}N ENDOR signals allowing accurate analysis of the magnetic interactions between the nitrogen nuclei and the high-spin center of Fe(III) in frozen-solution state.

Table 1. ^{14}N Hyperfine and Nuclear Quadrupole Coupling Constants of Aquometmyoglobin and Fluorometmyoglobin

Samples		Heme[a]		Proximal Histidine[b]	
		A_{33} (MHz)	$3P_{33}$ (MHz)	A_{zz} (MHz)	$3P_{zz}$ (MHz)
Mb^+	this work	7.52	-0.78	11.32	-3.44
	Crystal[c]	7.11 (av)	-0.81 (av)	11.55	-3.36
MbF (pH = 6)		7.66	-0.56	10.46	-3.68
MbF (pH = 11)		7.82	-0.56	10.12	-3.73

[a]The values are tensor components which are normal to the heme plane. Uncertainty for this work is ±0.15 MHz. av means average value of four heme nitrogens. Signs are adapted from ref. (2). [b]The values are tensor components which are along Fe-N_ε bond. Uncertainty for this work is ±0.15 MHz. [c]Data from ref. (2).

Upon fluorination, the ^{14}N hyperfine coupling (A_{zz}) is decreasing while the nuclear quadrupole coupling (Q_{zz}) is increasing for the histidine. This trend is reversed for the heme nitrogens. The ^{14}N hyperfine and nuclear quadrupole couplings for the heme and the histidine nitrogens are expressed as[2]

$$A_{33}(\text{heme}) = A_{iso} - (1-3\sin^2\beta)A_d + 2A_\pi - A_\sigma, \quad (5)$$
$$A_{zz}(\text{his}) = A_{iso} + 2A_d - A_\pi + 2A_\sigma, \quad (6)$$
$$P_{33}/P_o(\text{heme}) = -c/2(1-\cot^2\theta) - b/2(1+\cot^2\theta) + a. \text{ and} \quad (7)$$
$$P_{zz}/P_o(\text{his}) = c(1-\cot^2\theta) + b(\cot^2\theta - 1/2) - a/2. \quad (8)$$

Here, A_{iso}, A_d, $2A_\pi$, A_σ, and β are the Fermi contact term proportional to the electron-spin density in nitrogen 2s orbital, dipole-dipole interaction between the electron spin in Fe(III) and the nitrogen nuclear spin, dipolar interaction with the electron spin in nitrogen p_π orbital normal to the heterocyclic rings, dipolar interaction with the electron spin in nitrogen p_σ orbital for each nitrogen, and the out-of-planarity angle of iron. And a, b, and c of each nitrogen are electron populations in p_π orbital, each of two σ orbitals directed to adjacent carbons, and σ orbitals pointing the iron ion. 2θ is the angle of CNC. P_o is a proportionality relating the quadrupole parameters to electron density (P_0 = -4.5 MHz).

When Mb^- is fluorinated, the axial water ligand is replaced with fluoride ion. Structually, this brings minor perturbation in Fe-N distances and bond angles of heterocycles.[24] These changes are not big enough to explain the changes of

^{14}N couplings in eq's (5)-(8). One structurally noticeable change is the angle between the projection of the proximal histidine on the heme plane and the line of N1-N3 heme nitrogens.[25] The angle is changed from ~0° in Mb$^-$ to 20° in MbF.[24] Scholes *et al.* calculated the effect of the angle on the ^{14}N hyperfine and the nuclear quadrupole couplings. however. they found that the angle does not much affect the hyperfine and quadrupole couplings.[2] Hence. the structural changes are not the cause of the ^{14}N ENDOR changes.

The major contribution of $^{14}N_\varepsilon$ hyperfine coupling of the proximal histidine is σ-bonding to the metal d_{z^2} orbital (A_{iso}). Previous ^{19}F ENDOR showed that fluoride ion in MbF has ~1% of spin density in its 2s orbital at low pH.[4] At low pH in MbF. N_δ of the distal histidine is protonated and at high pH the proton is released. This changes the charge character of the imidazole ring toward neutral. ^{19}F ENDOR showed that this brings ~3% increase of the spin density on fluoride ion which is hydrogen-bonded to N_εH of the distal histidine.[4] From this point of view. one can expect reduction of the spin density on the 2s orbital of the histidine N_ε. *trans* ligand of fluoride which also have σ bonding to the metal d_{z^2} orbital. This is in good agreement with the observed change of hyperfine coupling constant of $^{14}N_\varepsilon$ of the proximal histidine. where A_{zz} decreases upon fluorination and ~3% reduction of A_{zz} in high pH (Table 1). However. the hyperfine coupling of the heme nitrogens is not much changed since they are σ-bonded to metal $d_{x^2-y^2}$ or d_{xy} orbitals which are normal to the d_{z^2} orbital. This indicates that electronegativity of fluoride ion affects the spin density mostly in iron d_{z^2} orbital not in other orbitals.

As in Table 1. the quadrupole coupling (P_{zz}) of the histidine N_ε is increasing upon fluorination and high pH form of MbF while that (P_{33}) of the heme nitrogens is decreasing. Though ^{14}N nuclear quadrupole coupling is sensitive to CNC angles of the histidine and pyrroles. it is expected that the angles are not much altered by fluorination and pH change. According to eq.'s (7) and (8). a is to be decreased or b and/or c are to be increased to increase P_{zz}/P_o for the histidine and to decrease P_{33}/P_o for the heme. In other words. the p_π orbital population of each nitrogen is increased or populations of p_σ orbitals are decreased. More quantitative discussion for this change is limited with current date and we are in underway to collect ^{14}N ENDOR across the EPR envelopes to extract full tensors of the hyperfine and nuclear quadrupole couplings.

Previous ^{19}F and ^{1,2}H ENDOR study of MbF in frozen-solution state provided sensitive tools sensing subtle structural changes of the heme that are not obtainable from X-ray.[4] Because of the intrinsic inhomogeneous line broadening effect of MbF in frozen-solution state. detection of the electronic and geometrical changes of the heme ring itself and the proximal histidine by using ^{14}N CW ENDOR was limited. In the present study. hyperfine-sensitive ^{14}N Mims ENDOR technique of pulsed-EPR was employed to probe the changes. With two different τ values of 128 and 196 ns. ^{14}N ENDOR signals of the heme and proximal histidine was almost completely resolved at $g'_{\|}$ (= g_e = 2). This study presents surprising results that the distal site of the heme sensitively affects the spin densities and p orbital populations of the proximal and the heme nitrogens. which can be readily detected by X-band Mims ENDOR sequence and that X-band Mims ^{14}N ENDOR provide a probe of structural and geometrical features of the heme and the proximal histidine.

Acknowledgment. This work has been supported by the Korea Research Foundation (KRF-2001-015-DP0251; HIL) and the National Institutes of Health (HL 13531: Brian M. Hoffman). Author thanks Dr. Judith M. Nocek for providing the samples and Prof. Brian M. Hoffman for helpful discussion.

References

1. Springer. B. A.; Sligar, S. G.; Olsen, J. S.; Phillips, G. N., Jr. *Chem. Rev.* **1994**, *94*, 699.
2. Scholes. C. P.; Lapidot. A.; Mascarenhas. R.; Inubushi. T.; Isaacson. R. A.; Feher. G. *J. Am. Chem. Soc.* **1982**. *104*. 2724.
3. Scholes. C. P.; Isaacson. R. A.; Feher. G. *Biochim. Biophys. Acta* **1971**. *244*. 206.
4. Fann. Y.-C.; Ong. J.-I.; Nocek. J. M.; Hoffman. B. M. *J. Am. Chem. Soc.* **1995**. *117*. 6019.
5. Feher. G.; Issacson. R. A.; Scholes. C. P.; Nagel. R. *Ann. N. Y. Acad. Sci.* **1973**. *222*. 86.
6. Mulks. C. F.; Scholes. C. P.; Dickinson. L. C.; Lapidot. A. *J. Am. Chem. Soc.* **1979**, *101*. 1645.
7. Mims. W. B. *Proc. R. Soc. London* **1965**. *283*. 452.
8. Antonini. E.; Brunori. M. *Hemoglobin and Myoglobin in Their Reactions with Ligands*: American Elsvier Publishing Co.: New York. 1971.
9. Werst. M. M.; Davoust. C. E.; Hoffman. B. M. *J. Am. Chem. Soc.* **1991**. *113*. 1533.
10. Mailer. C.; Taylor. C. P. S. *Biochim. Biophys. Acta* **1973**. *322*. 195.
11. Feher. G. *Phys. Rev.* **1959**. *114*. 1219.
12. Fan. C.; Doan. P. E.; Davoust. C. E.; Hoffman, B. M. *J. Magn. Reson.* **1992**, *98*, 62.
13. Gemperle. C.; Schweiger. A. *Chem. Rev.* **1991**. *91*. 1481.
14. Mims. W. B. *Proc. R. Soc. London* **1965**. *283*. 452.
15. Abragam. A.; Bleaney. B. *Electron Paramagnetic Resonance of Transition Ions*, 2nd ed.: Claren Press: Oxford. 1970.
16. Hoffman, B. M.; DeRose, V. J.; Doan, P. E.; Gurbiel. R. J.; Houseman. A. L. P.; Telser, J. *Biological Magnetic Resonance, Vol. 13: EMR of Paramagnetic Molecules*: Berliner. L. J., Reuben. J., Eds.: Plenum Press: New York. 1993.
17. True. A. E.; Nelson. M. J.; Venters. R. A.; Orme-Johnson. W. H.; Hoffman, B. M. *J. Am. Chem. Soc.* **1988**. *110*. 1935.
18. Kotani. M.; Morimoto, H. *Biochim. Biophys. Acta* **1966**. *126*. 176.
19. Kotani. M.; Morimoto. H. *Magnetic Resonance in Biological Systems*: Pergamon Press: New York. 1967.
20. Veselov. A. V.; Osborne. J. P.; Gennis. R. B.; Scholes. C. P. *J. Am. Chem. Soc.* **2000**. *122*. 8712.
21. ^{14}N ENDOR of Mb$^+$ crystal showed that the hyperfine couplings of four heme nitrogens are inequivalent.[2] However. ^{14}N ENDOR obtained from frozen-solution samples does not resolve the ENDOR lines of four heme nitrogens.
22. Doan. P. E.; Fan. C.; Hoffman, B. M. *J. Am. Chem. Soc.* **1994**. *116*. 1033.
23. Willems. J.-P.; Lee, H.-I.; Burdi. D.; Doan, P. E.; Stubbe. J.; Hoffman. B. M. *J. Am. Chem. Soc.* **1997**. *119*. 9824.
24. Bolognesi. M.; Onesti. S.; Gatti. G.; Ascenzi. P.; Brunori. M. *J. Mo. Biol.* **1989**. *205*. 529.
25. Here. N1 and N3 nitrogens belong to IV and II pyrrole rings. respectively.